APS physics

CHORUS

This is the accepted manuscript made available via CHORUS. The article has been published as:

Exact solutions for two-dimensional topological superconductors: Hubbard interaction induced spontaneous symmetry breaking

Motohiko Ezawa

Phys. Rev. B **97**, 241113 — Published 19 June 2018

DOI: 10.1103/PhysRevB.97.241113

Exact solutions in two-dimensional topological superconductors: Hubbard interaction induced spontaneous symmetry breaking

Motohiko Ezawa
Department of Applied Physics, University of Tokyo, Hongo 7-3-1, 113-8656, Japan

We present an exactly solvable model of a spin-triplet f-wave topological superconductor on the honeycomb lattice in the presence of the Hubbard interaction for arbitrary interaction strength. First we show that the Kane-Mele model with the corresponding spin-triplet f-wave superconducting pairings becomes a full-gap topological superconductor possessing the time-reversal symmetry. We then introduce the Hubbard interaction. The exactly solvable condition is found to be the emergence of perfect flat bands at zero energy. They generate infinitely many conserved quantities. It is intriguing that the Hubbard interaction breaks the time-reversal symmetry spontaneously. As a result, the system turns into a trivial superconductor. We demonstrate this topological property based on the topological number and by analyzing the edge state in nanoribbon geometry.

Introduction: Topological superconductors have been investigated intensively in this decade[1,2]. A particular feature is that they host Majorana fermions[3–5]. It is a crucial problem how the topological properties are affected by the presence of the interaction. It is in general a formidable task to attack this problem in strongly correlated systems. Nevertheless, if there are exactly solvable models, they are quite powerful since they provide us with a clear physical understanding. Exact solutions in one-dimensional Kitaev topological superconductors have been constructed[6–10]. On the other hand, as far as we are aware of, there are so far no exact solutions for higher dimensional topological superconductors.

A Kitaev spin liquid[11] on the honeycomb lattice is a beautiful example of the exact solvable model on interacting Majorana fermions. A key point is that two Majorana fermion operators are made C numbers on the basis of infinitely many conserved quantities present. Then the interacting Majorana fermion model is transformed into a free Majorana fermion model. It is recently shown that this method is also applicable to trivial BCS superconductors with the Hubbard interaction[12]. Explicit examples have been constructed for the square and cubic lattices.

In this paper, we investigate interacting two-dimensional topological superconductors on the honeycomb lattice. Our observation is that the exactly solvable condition is the emergence of perfect flat bands at zero energy. The operator degrees of freedom associated with the perfect flat bands become C-numbers, and generate infinitely many conserved quantities. The resultant Majorana fermion model is transformed into a free Majorana fermion model.

We explicitly analyze the Kane-Mele model with the spin-triplet f-wave superconductor, since the f-wave superconducting pairing is compatible with the honeycomb lattice structure [Fig.1]. We can tune this model so as to possess perfect flat bands at zero energy. The system becomes a full-gap superconductor. It is shown to be a time-reversal invariant topological superconductor by analytically evaluating the spin-Chern number. Next, we introduce the Hubbard interaction into this system. The system is still exactly solvable for arbitrary interaction strength. It is intriguing that the time-reversal symmetry is spontaneously broken by the choice of the ground state. This leads to the conclusion that the system becomes a trivial superconductor, which we confirm by analyzing the edge states of zigzag nanoribbons based on the bulk-edge correspondence.

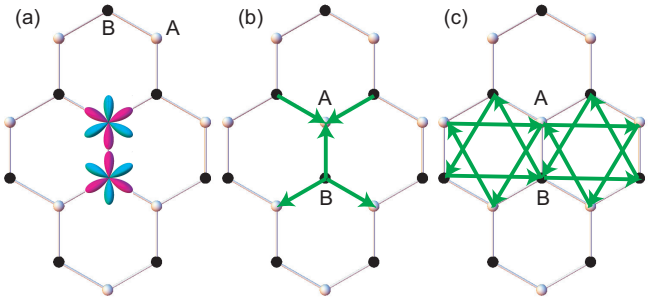

FIG. 1: (a) Illustration of the honeycomb lattice and the f-wave superconducting pairing. We see that the f-wave superconducting pairing is compatible with the honeycomb lattice. Superconducting pairings indicated by green arrows between (b) the nearest-neighbor sites and (c) the next-nearest neighbor sites. The sign is plus (minus) for the forward (backward) direction of the arrows. Arrows are pointing inside for A sites, while they are pointing outside for B sites in (b).

Model: We consider a model consisting of the Kane-Mele term[15] $H_{\rm KM}$ on the honeycomb lattice with the spin-triplet f-wave superconducting pairing term $H_{\rm SC}$ and the Hubbard interaction term $H_{\rm Hubbard}$. As shown in Fig.1, the f-wave superconducting pairing is compatible with the honeycomb lattice and is natural as well as the s-wave superconducting pairing. We assume an equal spin pairing. The total Hamiltonian is

$$H = H_{\rm KM} + H_{\rm SC} + H_{\rm Hubbard} \tag{1}$$

with

$$H_{\rm KM} = -t\sum_{\langle i,j\rangle s} c_{is}^\dagger c_{js} + i\frac{\lambda}{3\sqrt{3}}\sum_{\langle\langle i,j\rangle\rangle s}\nu_{ij}\sigma_z c_{is}^\dagger c_{js}, \tag{2}$$

$$H_{\rm SC} = -\Delta_1\sum_{\langle i,j\rangle s} c_{is}^\dagger c_{js}^\dagger + i\frac{\Delta_2}{3\sqrt{3}}\sum_{\langle\langle i,j\rangle\rangle s}\nu_{ij}\sigma_z c_{is}^\dagger c_{js}^\dagger + \text{h.c.}, \tag{3}$$

$$H_{\rm Hubbard} = U\sum_i\left(c_{i\uparrow}^\dagger c_{i\uparrow} - \frac{1}{2}\right)\left(c_{i\downarrow}^\dagger c_{i\downarrow} - \frac{1}{2}\right), \tag{4}$$

where $c_{is}^\dagger$ creates an electron with spin polarization s at site i,

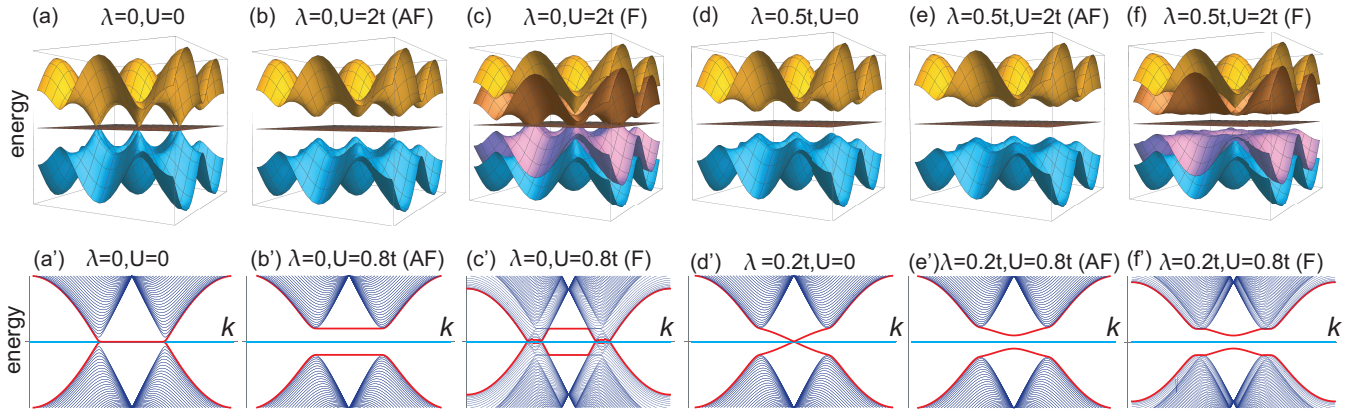

FIG. 2: (a)–(f) Bird's eye's views of the bulk band structures on the k_x-k_y plane, where (F) indicates the ferro-order, while (AF) indicates the antiferro-order. (a')–(f') Band structures of nanoribbons, where red curves represent the edge modes showing whether the system is trivial or topological. The system is topological (trivial) in the presence (absence) of edges modes connecting the conduction and valence bands. Cyan lines represent perfect flat bands. (a),(a') The system is a point-nodal superconductor without the Kane-Male term ($\lambda = 0$) and without the Hubbard interaction ($U = 0$). (b),(b') It is a trivial superconductor for $\lambda = 0$ and $U \neq 0$ due to the lack of such edge modes. (d),(d') It is a topological superconductor for $\lambda \neq 0$ and $U = 0$ due to the presence of such edge modes. (e),(e') It is a trivial superconductor for $\lambda \neq 0$ and $U \neq 0$ due to the disappearance of such edge modes. The energy of the antiferro-order is found to be lower than that of the ferro-order by comparing (b) and (c), and also by comparing (e) and (f). The vertical axis is the energy.

and $\langle i,j\rangle$ / $\langle\langle i,j\rangle\rangle$ run over all the nearest/next-nearest neighbor hopping sites. We adopt the convention that $s = \uparrow, \downarrow$ in indices and $s = +1, -1$ in equations for the up and down spins. We explain each term: (i) The first term of the Hamiltonian $H_{\rm KM}$ represents the usual nearest-neighbor hopping with the transfer energy. (ii) The second term of the Hamiltonian $H_{\rm KM}$ represents the Kane-Mele spin-orbit coupling, where $\sigma = (\sigma_x, \sigma_y, \sigma_z)$ is the Pauli matrix of spin, with $\nu_{ij} = +1$ if the next-nearest-neighboring hopping is anticlockwise and $\nu_{ij} = -1$ if it is clockwise with respect to the positive z axis. (iii) The first/second term of the Hamiltonian $H_{\rm SC}$ represents the nearest/next-nearest neighbor f-wave superconducting pairings. The system has the time-reversal symmetry.

We discuss a setup of the model Hamiltonian (1), where the spin-triplet f-wave topological superconductor emerges by way of the Kane-Mele spin-orbit interaction. First we note that the Kane-Mele model is realized in silicene, germane and stanene[26–29], which are monolayer materials of silicon, germanium and tin. Next, the spin-triplet f -wave superconducting pairing is induced by the Hubbard interaction in the Kane-Mele model[13,14] on the honeycomb lattice provided a certain doping is made. Then, we consider a system made of honeycomb layers in close proximity. The upper layer is the topological insulator described by the Kane-Mele term $H_{\rm KM}$ with the Hubbard term $H_{\rm Hubbard}$, upon which we focus. The lower layers form van der Waals hetro-structure of f -wave superconductor, which would induce the BCS pairing term[16] $H_{\rm SC}$ to the upper layer as a proximity effect. The effective Hamiltonian for the upper layer is given by (1).

Non-interacting case: First we investigate the non-interacting case; $U = 0$. The system has the time-reversal symmetry $T^{-1}H(\mathbf{k})T = H(-\mathbf{k})$ with $T = i\sigma_y K$, where K denotes the complex conjugation. Namely, the system is the time-reversal invariant superconductor belonging to the class DIII. The Hamiltonian is block diagonal with respect to the spin; $H = H_\uparrow + H_\downarrow$. In order to study superconductivity, we use the Bogoliubov de Gennes formalism. The honeycomb lattice is bipartite, which consists of the A and B sublattices. The nearest neighbor superconducting pairing occurs between the A and B sublattices, while the next-nearest neighbor superconducting pairing occurs within one sublattice: See Figs.1(b)–(c). The Nambu spinor consists of the electrons and holes, and reads $\Psi_s = \left(c_{As}(k), c_{Bs}(k), c^\dagger_{As}(-k), c^\dagger_{Bs}(-k)\right)$. In the Nambu spinor basis the Hamiltonian H_s has the form

$$H_s = \begin{pmatrix} s\lambda S & tF & -s\Delta_2 S & \Delta_1 F \\ tF^* & -s\lambda S & -\Delta_1 F^* & -s\Delta_2 S \\ -s\Delta_2 S & -\Delta_1 F & s\lambda S & -tF \\ \Delta_1 F^* & -s\Delta_2 S & -tF^* & -s\lambda S \end{pmatrix}, \tag{5}$$

with

$$F = e^{-iak_y/\sqrt{3}} + 2e^{iak_y/2\sqrt{3}} \cos\frac{ak_x}{2}, \tag{6}$$

$$S = \frac{2\lambda}{3\sqrt{3}}\left[\sin ak_x - \sin\left(\frac{ak_x}{2} + \frac{\sqrt{3}ak_y}{2}\right) - \sin\left(\frac{ak_x}{2} - \frac{\sqrt{3}ak_y}{2}\right)\right]. \tag{7}$$

We find $E = \pm\sqrt{(t-\Delta_1)^2|F|^2 + (\lambda-\Delta_2)^2 S^2}$ and $E = \pm\sqrt{(t+\Delta_1)^2|F|^2 + (\lambda+\Delta_2)^2 S^2}$ as the eigenvalues. It is remarkable that perfect flat bands emerge when

$$\Delta_1 = t, \qquad \Delta_2 = \lambda. \tag{8}$$

As we verify later, the emergence of perfect flat bands generates infinitely many conserved quantities and make one

species of the Majorana fermions inactive in the theory with the interaction ($U \neq 0$): See (17). In the following, we investigate the system by requiring the flat band condition (8). When $\lambda = 0$, the gap closes linearly at the K and K' points. It is a Dirac-nodal superconductor: See Fig.2(a). Once the λ becomes non-zero, the system becomes a full-gap superconductor: See Fig.2(d). We show that it is a topological superconductor by evaluating the topological numbers for $\lambda \neq 0$ and $U = 0$ [Fig.2(d)].

Topological numbers: The topological numbers are the Chern number $\mathcal{C}$ and the spin-Chern number $\mathcal{C}_\sigma$. The Chern number is zero, $\mathcal{C} = 0$, due to the time-reversal symmetry. The spin-Chern number $\mathcal{C}_\sigma$ is given by $\mathcal{C}_\sigma = (\mathcal{C}_\uparrow - \mathcal{C}_\downarrow)/2$ in terms of the spin-dependent Chern number $\mathcal{C}_s$ for each spin subsector[17–20]. We find that $\mathcal{C}_\sigma$ is zero for the flat bands since the eigen functions are given by $\Psi = (1, 0, 1, 0)$ and $\Psi = (0, -1, 0, 1)$ for them. In order to evaluate $\mathcal{C}_s$ for the valence band, we make Taylor expansions of (6) and (7) to find $F = \hbar v_{\rm F}(\xi k_x - i k_y)$ and $S = \xi\lambda$, where $v_{\rm F} = \frac{\sqrt{3}}{2\hbar}at$ is the Fermi velocity and $\xi = 1$ for the K point and $\xi = -1$ for the K' point. The Berry curvature is calculated as

$$\Omega_s(\mathbf{k}) = \nabla \times \mathbf{a}(\mathbf{k}) = \frac{s\lambda}{2}\left((\hbar v_{\rm F} k)^2 + \lambda^2\right)^{-3/2}, \qquad (9)$$

with the Berry connection $a_i(\mathbf{k}) = -i\langle\psi(\mathbf{k})|\frac{\partial}{\partial k_i}|\psi(\mathbf{k})\rangle$. The $\mathcal{C}_s$ is explicitly evaluated as

$$\mathcal{C}_s = \int \Omega_s(\mathbf{k})\, d^2\mathbf{k}/(2\pi) = \mathrm{sgn}(s\lambda)/2, \qquad (10)$$

and hence we obtain $\mathcal{C}_\sigma = \mathrm{sgn}(\lambda)$, by adding the contributions from the K and K' points. Consequently, the system is topological for $\lambda \neq 0$. We note that the Z_2 index is identical to the spin-Chern number provided that the time-reversal symmetry is present and that the spin is a good quantum number. We may explicitly confirm the Chern number, $\mathcal{C} = \mathcal{C}_\uparrow + \mathcal{C}_\downarrow = 0$, as required by the time-reversal symmetry.

Interacting case: It is in general a very hard task to solve the problem involving the Hubbard interaction $H_{\rm Hubbard}$, since it is not a quadratic interaction. However, it is recently proposed[12] that the Hubbard interaction can be rewritten in the quadratic form under the flat band condition (8), by applying the method[11] employed in the Kitaev spin liquid to a fermionic system.

We introduce Majorana fermion operators η and γ for each sublattice defined by

$$c_{is} = \eta_{is} + i\gamma_{is}, \qquad c_{is}^\dagger = \eta_{is} - i\gamma_{is}, \qquad (11)$$

$$c_{js} = \gamma_{js} + i\eta_{js}, \qquad c_{js}^\dagger = \gamma_{js} - i\eta_{js}, \qquad (12)$$

for fermions on $i \in A$ and $j \in B$ sublattices. The Hamiltonian (1) is rewritten in terms of these Majorana fermions as

$$H = H^{(1)} + H^{(2)} + H_{\rm Hubbard} \qquad (13)$$

with

$$H^{(1)} = 2i\sum_{\langle i,j\rangle s}[(\Delta_1 + t)\gamma_{is}\gamma_{js} + (\Delta_1 - t)\eta_{is}\eta_{js}], \qquad (14)$$

$$H^{(2)} = \frac{1}{6\sqrt{3}}\sum_{\langle\langle i,j\rangle\rangle s}\nu_{ij}\sigma_z[(\Delta_2 + \lambda)\gamma_{is}\gamma_{js} + (\Delta_2 - \lambda)\eta_{is}\eta_{js}], \qquad (15)$$

$$H_{\rm Hubbard} = U\sum_i (2i\eta_{i\uparrow}\gamma_{i\uparrow})(2i\eta_{i\downarrow}\gamma_{i\downarrow}). \qquad (16)$$

Since the time-reversal symmetry $\mathcal{T}$ acts as[21] $\mathcal{T}^{-1} i\eta_{i\uparrow}\eta_{i\downarrow}\mathcal{T} = -i\eta_{i\uparrow}\eta_{i\downarrow}$ and $\mathcal{T}^{-1} i\gamma_{i\uparrow}\gamma_{i\downarrow}\mathcal{T} = -i\gamma_{i\uparrow}\gamma_{i\downarrow}$, there exists the time-reversal symmetry in the interacting system (1).

By requiring the flat band condition (8), the Hamiltonian for the η Majorana fermions becomes exactly zero in Hamiltonians (14) and (15). It produces perfect flat bulk Majorana bands for the non-interacting system [Fig.2(a) and (d)]. They do not generate topological edges in nanoribbon geometry since the bulk topological quantum numbers are identically zero for the zero Hamiltonian [Fig.2(a') and (d')].

To explore the interacting system, we set $D_i = 2i\eta_{i\uparrow}\eta_{i\downarrow}$. Since D_i commutes with the Hubbard interaction (16), or $[D_i, H_{\rm M}] = 0$ for all sites i, D_i becomes a C number. It is given by $D_i = \pm 1/2$ by using the relation $D_i^2 = 1/4$. It is analogous to the honeycomb Kitaev spin liquid model[11]. Substituting D_i to (16), the total Hamiltonian becomes

$$H = 4it\sum_{\langle i,j\rangle s}\gamma_{is}\gamma_{js} + \frac{i\lambda}{3\sqrt{3}}\sum_{\langle\langle i,j\rangle\rangle s}\nu_{ij}\sigma_z\gamma_{is}\gamma_{js} - U\sum_i D_i(2i\gamma_{i\uparrow}\gamma_{i\downarrow}). \qquad (17)$$

The perfect flat bands for the η Majorana fermions are not affected by the interaction ($U \neq 0$): See Fig.2. This is because the η Majorana fermions decouple from the system and its Hamiltonian is zero under the flat band condition (8) even in the presence of the Hubbard interaction.

It is remarkable that the Hamiltonian (17) is exactly solvable for any fixed set of D_i, since it is quadratic in terms of the fermion operators γ. A set of D_i serves as infinitely many conserved quantities that make the system exactly solvable. In particular, the ground state is given by a certain set of D_i, which breaks the time-reversal symmetry spontaneously.

There are 2^N choices for the set D_i in the N site system. This is the same as in the Kitaev spin liquid system. In the Kitaev spin liquid system, exact diagonalizations for finite size clusters with the periodic boundary condition show that the ground state is uniform in the unit cell[11]. It is natural to expect a similar situation to occur also in the present model. There are two uniform states. One is the ferro-order where the sign of D_i is the same between the two sublattices $D_i = 1/2$, while the other is the antiferro-order where the sign of D_i is opposite between the two sublattices $D_i = (-1)^i/2$. The $D_i = 1/2$ and $D_i = -1/2$ are related by the interchange of U and $-U$.

By exactly diagonalizing (17), the eigenenergy is given by

$$E^2 = (t|F| \pm U/4)^2 + \lambda^2 S^2 \qquad (18)$$

for the ferro-order, and

$$E^2 = t^2 |F|^2 + \lambda^2 S^2 + U^2/16 \tag{19}$$

for the antiferro-order, where the spectrum is doubly degenerated. We find that the ground state is given by the antiferro-order, where the band gap is given by $\sqrt{\lambda^2 + U^2/16}$. See Supplemental Material for more details[31].

The gap closes for the ferro-order with $\lambda = 0$, describing a loop-nodal superconductor [Fig.2(c)]. On the other hand, the gap does not close for the ferro-order with $\lambda \neq 0$ [Fig.2(b)] and the antiferro-order with arbitrary λ [Fig.2(e) and (f)].

The spin-Chern number $\mathcal{C}_\sigma$ is no longer a good topological number once the Hubbard interaction is switched on and a particular choice of the ground state is made. Indeed, the time-reversal symmetry is broken due to the last term of Eq.(17) for a fixed value of D_i for i. The Z_2 index is also ill defined since the time-reversal symmetry is spontaneously broken. On the other hand, the Chern number is well defined and remains to be zero ($\mathcal{C} = 0$) even if the spin is no longer a good quantum number. We can check that the Chern numbers of the two valence bands are precisely canceled. We expect that there are no other topological numbers in the present system. Then, the system turns into a trivial superconductor without gap closing due to the symmetry breaking[22]. It is possible to confirm this by calculating the edge states in nanoribbon geometry based on the bulk-edge correspondence.

Edge states: In order to visualize whether the system is topological or not, we calculate the band structure for nanoribbon geometry: See Fig.2. The band structures resemble those of graphene[23] for $\lambda = 0$ [Fig.2(a')] and silicene[24,25] for $\lambda \neq 0$ [Fig.2(d')] with the sole difference being the emergence of perfect flat bands at zero energy. Silicene is a typical example of topological insulators. The criterion to judge the topological superconductor is the emergence of edge modes connecting the conduction and valence bands just as in the case of the topological insulator.

First, we investigate the case with $\lambda = 0$. There are partial flat bands connecting the K and K' points in addition to the perfect flat bands. These partial flat bands move away from zero energy once the interaction is introduced ($U \neq 0$) [Figs.2(b), (b'), (c) and (c')]. The bulk spectrum is fully gapped for the antiferro-order [Fig.2(b)], where the nanoribbon spectrum shows that the system is trivial [Fig.2(b')]. On the other hand, the bulk spectrum is gapless for the ferro-order [Fig.2(c) and (c')] apart from the perfect flat bands.

Next, we investigate the case with $\lambda \neq 0$. When $U = 0$, there are helical edge states connecting the conduction and valence bands [Fig.2(d')] in full-gap superconductor [Fig.2(d)], demonstrating that the system is topological. These helical edge states anticross once the interaction is introduced for both the antiferro-order [Fig.2(e')] and the ferro-order [Fig.2(f')], which implies that the system turns into a trivial superconductor for $U \neq 0$. This anticrossing can be understood in the low-energy continuum theory. The helical edge states are perfectly localized in one of the sublattices. The low-energy Hamiltonian is effectively given by

$$\begin{aligned} H_{\text{edge}} = & ivk[\gamma_\uparrow(k)\gamma_\uparrow(-k) - \gamma_\downarrow(k)\gamma_\downarrow(-k)] \\ & - iUD_i\gamma_\uparrow(k)\gamma_\downarrow(-k), \end{aligned} \tag{20}$$

where v is the velocity of the helical edge. The eigenenergy reads $E = \pm\sqrt{v^2k^2 + U^2}$. This effective Hamiltonian well describes the anticrossing of the helical edge states for both the ferro-order and the antiferro-order although their bulk spectra are different [Figs.2(e') and (f')].

A comment is in order with respect to the differences between the present work and the previous work[12]. The method is common, which is an application of the method used in the Kitaev spin liquid to a fermion system. The p-wave superconductor studied in Ref.[12] is actually a $p_x + p_y$ trivial superconductor. See Supplemental Material for details[31]. On the contrary, the present f-wave superconductor is topological due to the Kane-Mele spin-orbit interaction.

The present model is exactly solvable under the flat band condition (8), just as the $p_x + p_y$ model is[12]. Although it cannot be reached in realistic experiments, it is quite plausible that the results are adiabatically connected to an experimentally accessible region, as will be checked by future numerical simulations. The existence of exact solutions is very important to check numerical simulations, and it will motivate further studies on two dimensional topological superconductors.

The author is very much grateful to N. Nagaosa and Y. Tanaka for many helpful discussions on the subject. This work is supported by the Grants-in-Aid for Scientific Research from MEXT KAKENHI (Grant No. JP17K05490, and No. JP15H05854). This work is also supported by CREST, JST (JPMJCR16F1).

[1] X.-L. Qi, S.-C. Zhang, Rev. Mod. Phys. 83, 1057-1110 (2011).
[2] M. Sato and Y. Ando, Rep. Prog. Phys. 80, 076501 (2017).
[3] J. Alicea, Rep. Prog. Phys. 75, 076501 (2012).
[4] C. W.J. Beenakker, Annu. Rev. Condens. Matter Phys. 4, 113 (2013).
[5] S.R. Elliott and M. Franz, Rev. Mod. Phys. 87, 137 (2015).
[6] H. Katsura, D. Schuricht, and M. Takahashi, Phys. Rev. B 92, 115137 (2015).
[7] J.-J. Miao, H.-K. Jin, F.-C. Zhang, and Y. Zhou, Phys. Rev. Letters 118, 267701 (2017).
[8] M. Ezawa, Phys. Rev. B 96, 121105(R) (2017).
[9] M. McGinley, J. Knolle, and A. Nunnenkamp, Phys. Rev. B 96, 241113 (2017).
[10] Y. Wang, J.-J. Miao, H.-K. Jin, S. Chen, Phys. Rev. B 96, 205428 (2017)
[11] A. Kitaev, Annals of Physics 321, 2 (2006).
[12] Z. Chen, X. Li, and T. K. Ng, Phys. Rev. Lett. 120, 046401 (2018).
[13] L.-D. Zhang, F. Yang and Y. Yao, Sci. Rep. 5, 8203 (2015).
[14] Y. Fukaya, K. Yada, A. Hattori, and Y. Tanaka, J. Phys. Soc. Jpn. 85, 104704 (2016).

[15] C. L. Kane and E. J. Mele, Phys. Rev. Lett. **95**, 226801 (2005); ibid **95**, 146802 (2005).
[16] L.-Y. Xiao, S.-L. Yu, W. Wang, Z.-J. Yao and J.-X. Li, EPL 115, 27008 (2016).
[17] L. Sheng, D. N. Sheng, C. S. Ting, and F. D. M. Haldane, Phys. Rev. Lett. 95, 136602 (2005).
[18] D. N. Sheng, Z. Y. Weng, L. Sheng and F. D. M. Haldane, Phys. Rev. Lett. 97 036808 (2006).
[19] Y. Yang, Z. Xu, L. Sheng, B. Wang, D.Y. Xing, and D. N. Sheng, Phys. Rev. Lett. 107, 066602 (2011).
[20] M. Ezawa, J. Phys. Soc. Jpn. 84, 121003 (2015).
[21] X.-L. Qi, T. L. Hughes, S. Raghu, and S.-C. Zhang, Phys. Rev. Lett. 102, 187001 (2009).
[22] M. Ezawa, Y. Tanaka and N. Nagaosa, Scientific Reports 3, 2790 (2013).
[23] M. Ezawa, Physical Review B, 73, 045432 (2006).
[24] M. Ezawa, New J. Phys. 14, 033003 (2012).
[25] M. Ezawa, J. Phys. Soc. Jpn. 84, 121003 (2015).
[26] C.-C. Liu, W. Feng, and Y. Yao, Phys. Rev. Lett. **107**, 076802 (2011).
[27] C.-C. Liu, H. Jiang, and Y. Yao, Phys. Rev. B, **84**, 195430 (2011).
[28] M. Ezawa, J. Phys. Soc. Jpn. 84, 121003 (2015),
[29] M. Ezawa, Phys. Rev. Lett 109, 055502 (2012),
[30] E. H. Lieb, Phys. Rev. Lett. 73, 2158 (1994).
[31] See Supplemental Material at [URL] for a study of the $p_x + p_y$ model on the square lattice to see that it describes a trivial superconductor.